IMMUNOLOGY

Genome-wide RNAi screening implicates the E3 ubiquitin ligase Sherpa in mediating innate immune signaling by Toll in *Drosophila* adults

Hirotaka Kanoh,[1*†] Li-Li Tong,[1†] Takayuki Kuraishi,[1,2†‡§] Yamato Suda,[1] Yoshiki Momiuchi,[1] Fumi Shishido,[1] Shoichiro Kurata[1§]

The *Drosophila* Toll pathway plays important roles in innate immune responses against Gram-positive bacteria and fungi. To identify previously uncharacterized components of this pathway, we performed comparative, ex vivo, genome-wide RNA interference screening. In four screens, we overexpressed the Toll adaptor protein dMyd88, the downstream kinase Pelle, or the nuclear factor κB (NF-κB) homolog Dif, or we knocked down Cactus, the *Drosophila* homolog of mammalian inhibitor of NF-κB. On the basis of these screens, we identified the E3 ubiquitin ligase Sherpa as being necessary for the activation of Toll signaling. A loss-of-function *sherpa* mutant fly exhibited compromised production of antimicrobial peptides and enhanced susceptibility to infection by Gram-positive bacteria. In cultured cells, Sherpa mediated ubiquitylation of dMyd88 and Sherpa itself, and Sherpa and *Drosophila* SUMO (small ubiquitin-like modifier) were required for the proper membrane localization of an adaptor complex containing dMyd88. These findings highlight a role for Sherpa in *Drosophila* host defense and suggest the SUMOylation-mediated regulation of dMyd88 functions in Toll innate immune signaling.

INTRODUCTION

The fruit fly *Drosophila melanogaster* is a sophisticated model organism for which there are several genetic tools that enable the direct identification of genes responsible for various functions in vivo. Ex vivo, large-scale analyses have also contributed to the identification of many factors based on highly developed RNA interference (RNAi) technologies and numerous cell lines established from various fly organs (*1*–*3*).

The innate immune system is the frontline of the self-defense system against microbial infection in metazoan animals. In *Drosophila*, the production of antimicrobial peptides is a major effector mechanism for eliminating pathogenic microbes (*4*). At least two signaling pathways are involved in inducing the expression of genes that encode antimicrobial peptides: the Toll and Imd pathways (*5*). Upon infection by Gram-negative bacteria, peptidoglycan recognition protein LC (PGRP-LC) or PGRP-LE, the transmembrane or intracellular pattern recognition receptors for diaminopimelic acid (DAP)–type peptidoglycans released from Gram-negative bacteria (*6*–*8*) are activated and recruit Imd, an adaptor protein for PGRP-LC and PGRP-LE and a *Drosophila* counterpart of the mammalian receptor-interacting protein kinase 1 (RIPK1) (*9*). The caspase-8–like protein Dredd cleaves the Imd protein to form a signaling complex containing the E3 ubiquitin ligase Diap2 and E2 ubiquitin–conjugating enzymes, which is followed by K63-type polyubiquitylation of Imd (*10*). The signaling complex modified by polyubiquitin then activates transforming growth factor–β–activated kinase 1 (TAK1) and TAK1-binding protein 2 (TAB2), which leads to activation of the *Drosophila* inhibitor of κB (IκB) kinase (IKK) complex, which consists of the *Drosophila* IKKβ homolog ird5 and the IKKγ homolog kenny (*10*). The IKK complex then phosphorylates Relish, a *Drosophila* homolog of nuclear factor κB (NF-κB), which contains the transcription factor module in its N-terminal region and an autoinhibitory domain similar to IκB in its C-terminal region (*11*). The phosphorylated Relish protein is cleaved by Dredd, and the N-terminal transcription factor module of Relish translocates to the nucleus and induces the expression of genes that encode antimicrobial proteins, including *Diptericin* (*12*). The Imd pathway is essential for defense against Gram-negative bacteria (*5*).

The Toll pathway, on the other hand, is crucial for defense against fungal and Gram-positive bacterial infections (*5*). Infections by both fungi and Gram-positive bacteria stimulate serine protease cascades in the hemolymph, which result in the production of a cleaved form of the cytokine-like protein Spätzle (Spz), a ligand of Toll (*13*–*15*). Binding of the cleaved Spz to the ectodomain of Toll induces receptor dimerization (*16*). The dimerized Toll recruits a plasma membrane–associated complex consisting of dMyd88, the adaptor protein for the Toll receptor, which is homologous to the mammalian myeloid differentiation factor 88 (MyD88), and Tube, the *Drosophila* homolog for the mammalian interleukin-1 receptor (IL-1R)–associated kinase 4 (IRAK4) (*17*–*19*). Pelle, a serine and threonine kinase that is similar to the mammalian kinase IRAK1, is thought to be recruited to the signaling complex by Tube (*20*). Formation of this complex is thought to lead to the phosphorylation of Cactus, a *Drosophila* homolog of IκB, which binds to and inhibits Dif, another *Drosophila* homolog of NF-κB. Phosphorylated IκB undergoes degradation by the ubiquitin-proteasome system (*21*, *22*), leading to the release of Dif (*23*), which is followed by its entry into the nucleus to activate the transcription of genes encoding antimicrobial factors, such as the antifungal peptide gene *Drosomycin* (*24*).

The Toll-like receptor (TLR) signaling pathway is a major innate immune pathway in mammals. TLR signaling occurs through two distinct pathways that depend on the adaptor molecules MyD88 and TRIF (Toll/IL-1R domain–containing adaptor-inducing interferon-β) (*25*). The

[1]Division of Molecular Genetics, Graduate School of Pharmaceutical Sciences, Tohoku University, Sendai 980-8578, Japan. [2]Precursory Research for Embryonic Science and Technology (PRESTO), Japan Science and Technology Agency, Tokyo 102-0076, Japan.
*Present address: Division of Glycopathology, Institute of Molecular Biomembrane and Glycobiology, Tohoku Pharmaceutical University, Sendai 981-8558, Japan.
†These authors contributed equally to this work.
‡Present address: Department of Microbiology and Immunology, Keio University School of Medicine, Tokyo 160-8582, Japan.
§Corresponding author. E-mail: takayuki.kuraishi@gmail.com (T.K.); kurata@mail.pharm.tohoku.ac.jp (S.K.)

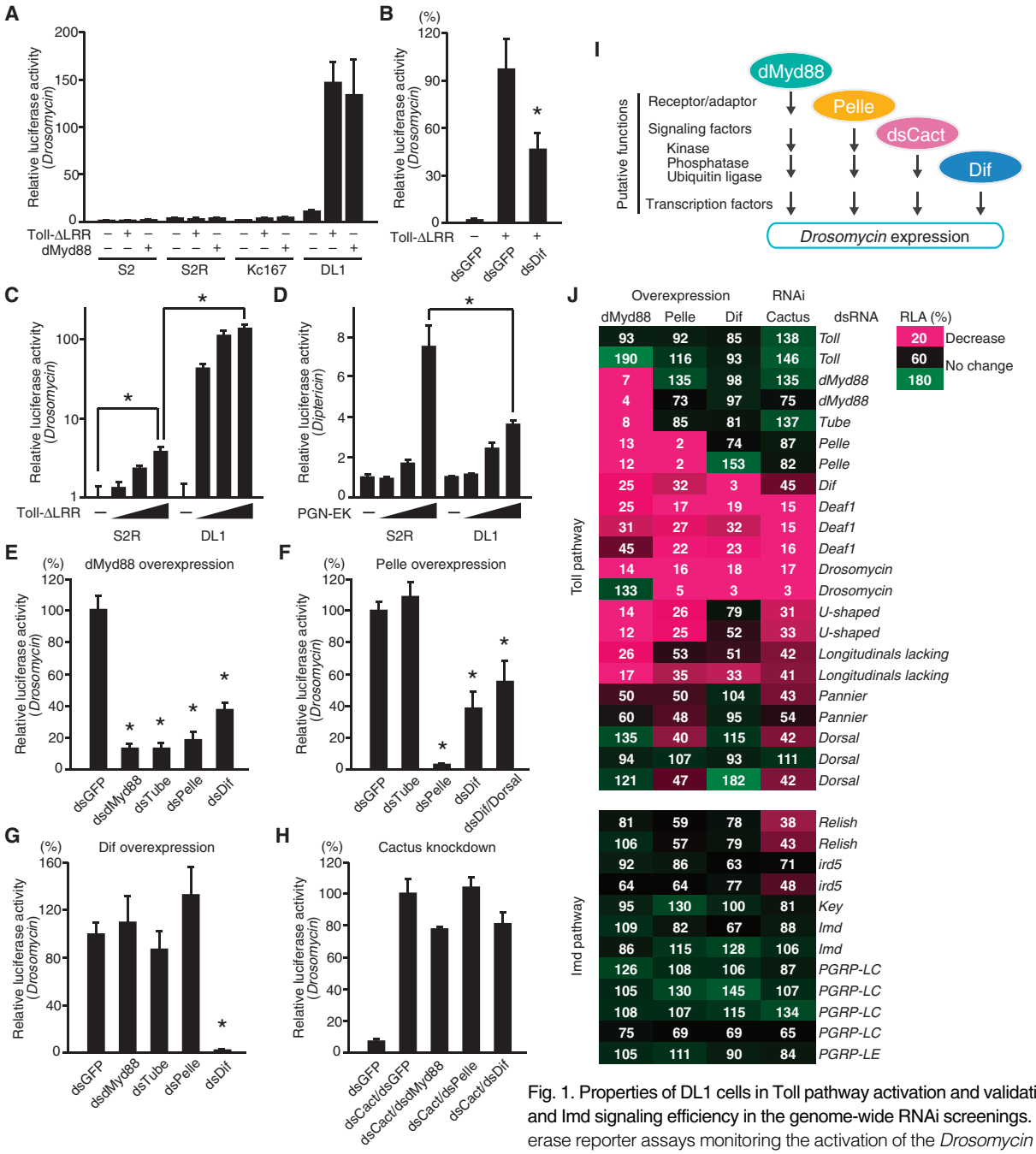

Fig. 1. Properties of DL1 cells in Toll pathway activation and validation of Toll and Imd signaling efficiency in the genome-wide RNAi screenings. (**A**) Luciferase reporter assays monitoring the activation of the *Drosomycin* promoter were performed in the indicated cell lines, which were transfected with the *Drs*-luc reporter plasmid and with expression plasmids encoding either dMyd88 or Toll-ΔLRR, as indicated. (**B**) Relative luciferase activity (RLA) was measured in DL1 cells transfected with an expression plasmid encoding Toll-ΔLRR together with plasmids encoding dsGFP or dsDif. (**C** and **D**) S2R and DL1 cells were transfected with increasing amounts of plasmids encoding Toll-ΔLRR (C) or PGN-EK (D) and then were subjected to luciferase assays to compare the extents of Toll signaling (C) and Imd signaling (D). (**E** to **H**) RLA was assessed in DL1 cells transfected with plasmids encoding dMyd88 (E), Pelle (F), or Dif (G) for overexpression or encoding Cactus-specific double-stranded RNA (dsRNA) for knockdown (H) together with the indicated dsRNAs. dsGFP was used as a negative control. Data in (A) to (H) are means ± SEM of triplicate wells from a single experiment and are representative of two independent experiments. $^*P < 0.05$ by Student's *t* test. (**I**) Concept behind the comparative genome-wide RNAi screen. Four distinct stimuli and the putative functions of target genes are represented in the signaling map of the Toll pathway. (**J**) Heat map of the RLA in cells overexpressing or deficient in known signaling components in the Toll and Imd pathway. The percentage RLA relative to the median is shown with a colored background. Red indicates 20% of median RLA, whereas black and green indicate changes in the range from 60 to 180% of the median RLA. More than one dsRNA amplicon was used for those genes that appear more than once.

MyD88-dependent signaling pathway is a hybrid of the *Drosophila* Toll and Imd pathways. With MyD88 adaptor–like (Mal) as a bridging molecule between TLRs and MyD88, activated TLRs recruit a signaling complex consisting of MyD88 and IRAK4, a serine and threonine kinase that contains an N-terminal death domain and is a counterpart to the *Drosophila* Tube. IRAK4 activates other IRAK family members, including IRAK1 and IRAK2 (*26*), which are mammalian homologs of *Drosophila* Pelle. The IRAKs then dissociate from MyD88 and interact with tumor necrosis factor (TNF) receptor–associated factor 6 (TRAF6), which acts as an E3 ubiquitin ligase. TRAF6 then activates TAK1, which phosphorylates IKKβ. Subsequently, the IKK complex, which consists of IKKα, IKKβ, and NEMO (also known as IKKγ), phosphorylates IκBα, thereby freeing NF-κB and enabling it to translocate into the nucleus (*27*).

The intracellular components of the *Drosophila* Toll signaling pathway are poorly characterized compared to the mammalian TLR and *Drosophila* Imd signaling pathways, which share downstream components as orthologs. For example, the signal-dependent regulation of Cactus degradation downstream of the kinase Pelle and the possible involvement of post-translational modifications, such as ubiquitylation and phosphorylation, are unclear. Here, we investigated the intracellular mechanism that controls the activation of the *Drosophila* Toll pathway based on an optimal cell line and strategic genome-wide RNAi screenings. We demonstrated that Sherpa is a previously uncharacterized component of the Toll pathway that is required for host defense in adult flies. Biochemical analyses suggested that Sherpa acted as an E3 ubiquitin ligase to mediate posttranslational modifications of dMyd88 and Sherpa itself, and we found that Sherpa and the *Drosophila* small ubiquitin-like modifier (SUMO) led the dMyd88-Tube complex to the appropriate subcellular compartment, which was indispensable for Toll-dependent innate immune signaling.

RESULTS

Drosophila DL1 cells: A suitable cell line for analyzing the intracellular Toll pathway

Ex vivo RNAi screening is a potentially useful method for clarifying the signaling components in the intracellular Toll pathway, because improper signaling of this pathway has lethal effects on fly development (*28*). Despite many attempts, only a few factors in the Toll pathway have been identified to date. In general, ex vivo studies of the *Drosophila* innate immune response are performed in *Drosophila* S2 cells, a macrophage-like cell line; however, S2 cells exhibit low responsiveness to stimulation of the Toll pathway, such as through the expression of active form of the Toll receptor (Toll-ΔLRR) (*6*), and considerable dependency on the Imd pathway for Toll pathway activation (*6*, *29*).

Therefore, to identify signaling factors that were previously unknown components of the intracellular Toll pathway, we first established a suitable cell line for studying the Toll pathway. We tested several cell lines, including S2, S2R, Kc167, and DL1 cells, with reporter assays with *Drosomycin* luciferase (*Drs*-luc), a firefly luciferase reporter construct with the promoter sequence of *Drosomycin*, an antimicrobial peptide gene that is specifically regulated by the Toll signaling pathway (*24*). To activate the Toll pathway, we transfected the cells with expression vectors encoding *Drosophila* MyD88 (dMyd88) or Toll-ΔLRR with a lipid-based transfection reagent that was compatible with the subsequent large-scale screening. The reporter assay revealed that the activation of the Toll pathway was 50-fold greater in the transfected DL1 cells compared with that in the other cell lines (Fig. 1A). Activation of the Toll pathway by overexpression of Toll-ΔLRR in DL1 cells was substantially inhibited by knockdown of Dif (Fig. 1B), an NF-κB–related transcription factor that is mainly involved in the innate immune response (*23*), which was suggestive of a dependency on the canonical Toll pathway in DL1 cells. Furthermore, we compared the signaling efficiency of the Toll and Imd pathways in S2R and DL1 cells. Toll pathway activation was substantially activated in S2R cells by overexpression of Toll-ΔLRR, but Toll pathway activation was enhanced in DL1 cells transfected with the same amount of the Toll-ΔLRR expression plasmid (Fig. 1C). On the other hand, the extent of Imd pathway activation in S2R cells in response to peptidoglycans derived from Gram-negative bacteria (as monitored by measurement of *Attacin* luciferase activity) was greater than that in similarly stimulated DL1 cells (Fig. 1D). These findings suggested the preferential activation of the Toll pathway relative to that of the Imd pathway in DL1 cells.

We then used an epistasis assay to confirm the contributions of intracellular components of the canonical Toll pathway activation in DL1 cells. We potentiated Toll pathway activation by overexpressing intracellular components such as dMyd88, Pelle, and Dif, and then measured the contribution of each signaling component to the pathway by measuring the effect of their knockdown. Toll pathway activation induced by the overexpression of dMyd88 was decreased by knockdown of dMyd88, Tube, Pelle, or Dif to 15 to 40% compared to that in cells treated with dsRNA specific for green fluorescent protein (GFP; Fig. 1E). The enhanced activation of the Toll pathway caused by overexpression of Pelle was not affected by knockdown of dMyd88 or Tube but was substantially decreased by knockdown of Pelle, Dif, or a combination of Dif and Dorsal (Fig. 1F). Knockdown of the signaling components upstream of Dif had no substantial effect on the enhanced Toll pathway activation that resulted from overexpression of Dif (Fig. 1G). These findings indicate that the signaling hierarchy of the Toll pathway is rigidly maintained in DL1 cells and that the contribution of intracellular components in the canonical pathway is substantial. In addition, we tested Toll pathway activation by knockdown of Cactus, an NF-κB inhibitory protein. Knockdown of Cactus potentiated activation of the Toll pathway (Fig. 1H), suggesting that Cactus also regulates the Toll signaling pathway in DL1 cells.

Genome-wide RNAi screening for Toll pathway activation in *Drosophila* DL1 cells

On the basis of the favorable properties of DL1 cells for these experiments, we performed large-scale screening for previously uncharacterized signaling components in the intracellular Toll pathway. We established a reporter-based screening system with 384-well microplates with the help of the *Drosophila* RNAi Screening Center (DRSC). We next performed a comparative genome-wide screening that consisted of four distinct screens (Fig. 1I). Through this process, we screened the Toll pathway by overexpression of dMyd88, Pelle, or Dif, as well as by knockdown of Cactus to cover a wide range of intracellular signaling events.

As a benchmark, we first analyzed defects in the activation of the Toll pathway by knocking down known signaling factors in the Toll and Imd pathways and comparing the RLAs in these cells to those of cells in which genes of interest were knocked down (Fig. 1J). Data obtained from these screens indicated that the signaling hierarchy of the Toll pathway was tightly regulated by its dependency on the two distinct innate immune signaling pathways in DL1 cells. Notably, knockdown of the NF-κB–like transcription factor Dif, which is required for *Drosomycin* expression in response to microbial infection in adult flies, inhibited *Drs*-luc activity, but knockdown of Dorsal, which is activated by the Toll pathway during embryogenesis (*30*), did not (Fig. 1J), suggesting that DL1 cells reflect the situation in the Toll pathway of *Drosophila* adults.

In all screening conditions, deformed epidermal autoregulatory factor 1 (Deaf1), a nuclear protein that acts downstream of Dif (*31*, *32*), was critically involved in the activation of the *Drosomycin* promoter (Fig. 1J). The proteins

A

Screen						
dMyd88	Pelle	dsCact	Dif	dsRNA	Function	RLA(%)
14	98	67	67	*CG9153*	E3	20 Decrease
17	110	56	128	*CG42593*	E3	60 No change
21	98	65	86	*CG42593*	E3	180
33	55	68	134	*Aos1*	SUMO E1	
44	51	81	58	*Aos1*	SUMO E1	
44	80	105	116	*Uba2*	SUMO E1	
52	87	112	112	*Ubc9*	SUMO E2	
61	89	112	100	*Ubc9*	SUMO E2	
93	65	88	99	*Uba1*	Ubiquitin E1	
119	93	130	93	*Uba3*	Ubiquitin E1	
18	48	118	157	*Smt3*	SUMO	
54	51	44	49	*Ubl*	Ubiquitin-like protein	
59	63	75	32	*CG33223*	Ubiquitin-like protein	
94	79	70	90	*Ub-p63E*	Ubiquitin	

B

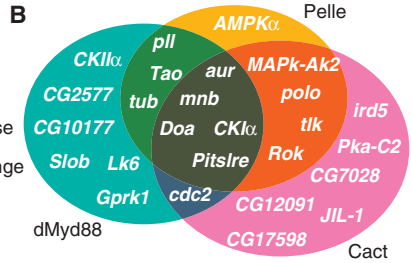

C

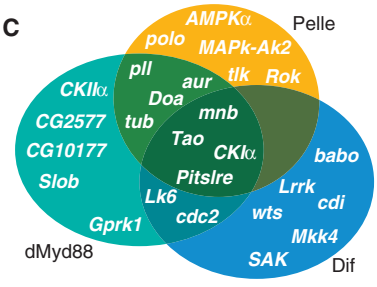

D

Screen				
dMyd88	Pelle	Cact	Dif	dsRNA
8	85	81	137	*tub*
12	2	82	153	*pll*
13	2	87	74	*pll*
2	26	37	57	*Doa*
143	35	23	90	*Doa*
19	30	30	52	*aur*
25	35	17	34	*PitsIre*
27	48	43	74	*PitsIre*
29	34	46	46	*mnb*
10	30	80	23	*Tao*
27	54	95	35	*Tao*
31	64	15	38	*cdc2*
30	76	26	53	*cdc2*
27	94	26	131	*Lk6*
15	44	92	117	*CKIα*
15	49	82	39	*CKIα*
73	80	46	175	*CKIα*

Fig. 2. Identification of possible ubiquitin- and SUMO-related factors and protein kinases. (**A**) Heat map comparison of the RLA values of cells transfected with dsRNAs targeting the E3 ubiquitin ligases encoded by *CG9153* and *CG42593* and the SUMO homolog encoded by *Smt3* in each screen (single replica) and those of cells transfected with dsRNAs targeting other E2 and E1 enzymes and ubiquitin-like modifiers. (**B** and **C**) Gene symbols of candidate genes encoding protein kinases that satisfied the criteria of each screen are indicated and compared in the Venn diagram. (**D**) Heat map comparison of the RLA values of cells in each screen transfected with dsRNAs targeting the indicated candidate kinase-encoding genes. In the heat map, red indicates a decrease in RLA to 20%, whereas black and green indicate no change in the range from 60 to 180%. More than one dsRNA amplicon was used for those genes that appear more than once in the list.

Pannier and U-shaped, the *Drosophila* GATA homolog and Friend of GATA protein, respectively, which are involved in hematopoiesis (*33*) and Toll signaling (*29*), also contributed to activation of the *Drosomycin* promoter in DL1 cells (Fig. 1J). Additionally, longitudinals lacking (Lola), a neuronal transcription factor with the domain organization of GATA factors, affects Toll pathway activation (*34*). Moreover, activation of the Toll pathway because of the knockdown of *Cactus* was strongly dependent on Deaf1 and broadly dependent on transcription factors in both the Toll and Imd pathways: Dif, Dorsal, and Relish (Fig. 1J). This finding suggested that the depletion of Cactus could induce the activation of comprehensive transcription factors related to both the Toll and Imd pathways.

Classification of putative candidate genes by functional annotation

On the basis of the RLA values of known signaling factors, we set criteria for each screen to judge potential candidate genes. In the dMyd88 screen, we collected first-hit genes with an RLA value that was <40% of the median RLA in each assay plate and normal cell viability (about 50 to 300% of the median *Renilla* luciferase activity in each assay plate). Next, we constrained the candidate genes to 111 by omitting housekeeping genes, such as those encoding basic transcription factors, translation factors, and ribosomal proteins, as well as weak hits (those with RLA values of 30 to 40%). In the screens for Pelle, Cactus, and Dif, genes whose knockdown resulted in RLA values of <50% of controls were judged as first hits, and then genes with low (<50%) or high (>200%) cell viability were omitted. On the basis of these criteria, we constrained the candidate genes to 258 in the Pelle screen, 310 in the Cactus screen, and 220 in the Dif screen.

To classify those candidate genes by their putative functions, we then categorized the candidate genes of each screen into between 9 and 15 functional annotation clusters (fig. S1 and data file S1) using The Database for Annotation, Visualization and Integrated Discovery (DAVID) bioinformatics resources 6.7 (*35*, *36*) and subsequent manual editing based on gene information from the National Center for Biotechnology Information (NCBI). Graphs of functional annotation clusters in each screen (fig. S1) showed that most of the candidate genes could be categorized into common clusters that included basic cell processes and putative signaling functions and domains: transcription, translation, and mRNA; the Toll signaling pathway; protein kinase and phosphatase; ubiquitin; transcription regulation; signaling; membrane protein; cytoskeleton; and zinc finger protein, among others. Many small sets of genes were included in the "other functions" group. Of these, we focused on enzymes required for post-translational modifications, such as phosphorylation and ubiquitylation, which may be involved in putative signaling mechanisms of the intracellular Toll pathway.

Involvement of an E3 ubiquitin ligase and protein kinase genes in Toll pathway signaling

First, we analyzed the candidate genes related to the ubiquitin system. Among the 111 positive genes in the dMyd88 screen, RNAi-mediated knockdown of suppressor of mif two 3 (Smt3)/SUMO (CG4494) and CG9153, designated Sherpa [SUMO-related HECT (homologous to the E6-AP carboxyl terminus) domain and RCC (regulator of chromosome condensation) repeat protein for Toll pathway activation], which encodes a HECT-type E3 ubiquitin ligase, exhibited the most substantial inhibition of *Drs*-luc activity (Fig. 2A). Our analysis indicated that knockdown of the SUMO E1-activating enzymes Aos1 and Uba2, as well as the SUMO E2 enzyme Ubc9, moderately inhibited Toll pathway activation induced by dMyd88 overexpression (Fig. 2A). Knockdown of these factors preferentially inhibited the dMyd88-mediated activation of the Toll pathway activation but had no effect on Toll pathway activation in cells in the other screens. These findings suggested that the E3 ubiquitin ligase Sherpa/CG9153 and SUMOylation factors mediate Toll pathway signaling

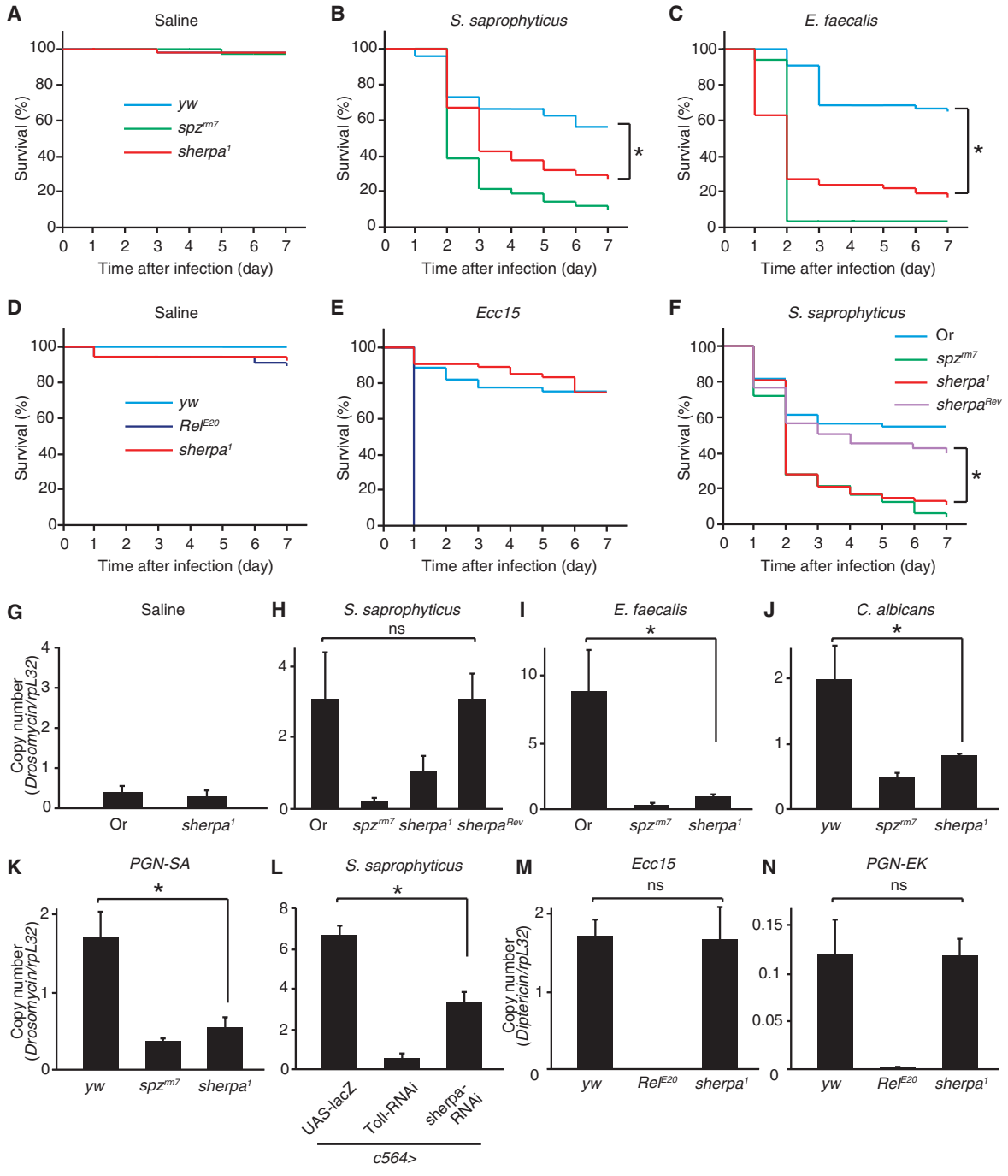

Fig. 3. Sherpa is required for host defense against Gram-positive bacterial and fungal infections. (A to F) The percentage survival rates of *sherpa*^{1} flies injected with saline (A and D), *Staphylococcus saprophyticus* (B and F), *Enterococcus faecalis* (C), and *Ecc15* (E) were compared with those of *yellow white* (*yw*) flies and *sherpa*^{Rev} files, as well as with flies with mutations in either the Toll pathway (*spz*^{rm7}) or the Imd pathway (*Rel*^{E20}). Data are representative of two (A and D) or more than three (B, C, E, and F) independent experiments with ~30 flies in each experiment. *$P < 0.05$ by log-rank test. (G to N) Analysis of the expression of genes encoding antimicrobial peptides in *sherpa* mutants. The relative abundances of *Drosomycin* (G to L) and *Diptericin* (M and N) mRNAs were determined by qPCR analysis of total RNA extracted from wild-type, *spz*^{rm7}, *Rel*^{E20}, *sherpa*^{1}, *sherpa*^{Rev}, *c564>lacZ* (*UAS-Dcr2/+;c564-GAL4/UAS-lacz*), *c564>Toll-RNAi* (*UAS-Dcr2/+;c564-GAL4/UAS-Toll-RNAi*), and *c564>sherpa-RNAi* (*UAS-Dcr2/+;c564-GAL4/UAS-sherpa-RNAi*) flies. The RNA samples were collected at 24 hours (G to I, K, and L), 18 hours (J), or 6 hours (M and N) after the flies were injected with saline (G), *S. saprophyticus* (H and L), *E. faecalis* (I), *Candida albicans* (J), PGN-SA (peptidoglycan from *Staphylococcus aureus*) (K), *Ecc15* (M), or PGN-EK (peptidoglycan from Escherichia coli) (N). Data in (G) to (N) are representative of more than three independent experiments each performed in triplicate (10 flies ×3). *$P < 0.05$ by Student's *t* test. Or, Oregon R strain; ns, not significant.

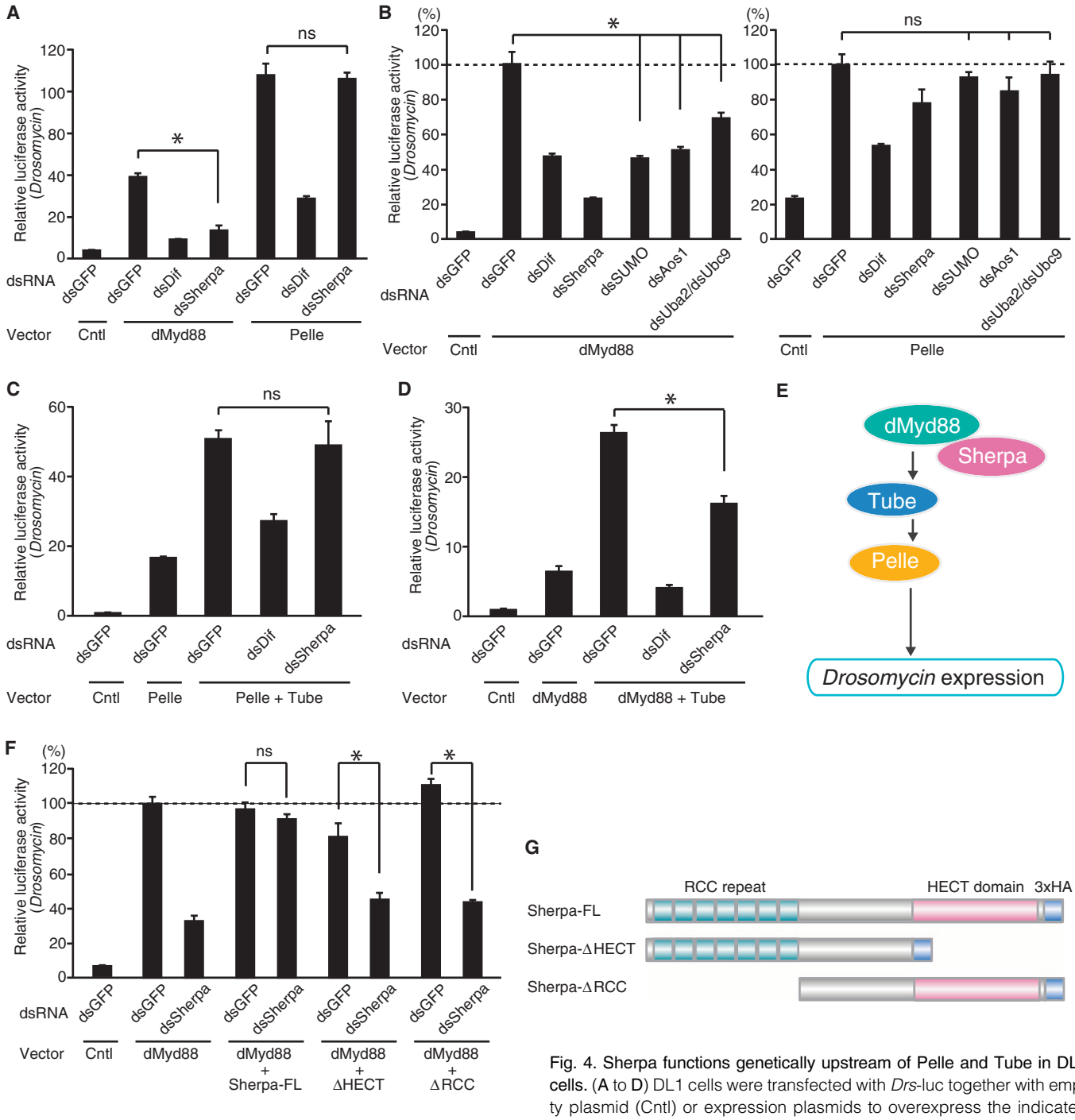

Fig. 4. Sherpa functions genetically upstream of Pelle and Tube in DL1 cells. (**A** to **D**) DL1 cells were transfected with *Drs*-luc together with empty plasmid (Cntl) or expression plasmids to overexpress the indicated combinations of proteins and dsRNAs before being subjected to luciferase reporter assays. (**E**) Schematic representation of Toll signaling and the genetic interaction of *sherpa*. (**F**) DL1 cells were transfected with the *Drs*-luc reporter and plasmid expressing dMyd88 together with plasmids encoding full-length Sherpa (Sherpa-FL), Sherpa-ΔHECT, or Sherpa-ΔRCC, as well as with dsRNA targeting GFP or the 5′UTR of Sherpa before being analyzed to determine luciferase activity. (**G**) Schematic representation of the protein structure of Sherpa. Seven RCC repeats whose function is unknown reside in the N terminus of Sherpa, and the HECT domain required for its E3 ubiquitin ligase activity is located at the C terminus of the protein. The 3×HA tag was added to the C terminus of Sherpa. Mutant Sherpa proteins devoid of the HECT domain or the RCC repeat are shown. Data in (A) to (D) and (F) are means ± SEM of triplicate samples from a single experiment and are representative of two (D), three (B, C, and F), and four (A) independent experiments. *$P < 0.05$ by Student's *t* test.

downstream of or in parallel to dMyd88. Furthermore, we also identified CG42593/Ubr3, which encodes a really interesting new gene (RING)–type E3 ligase that functions with the E3 ubiquitin ligase Diap1 in apoptotic pathways (*37*), as a strong hit in the dMyd88 screen (Fig. 2A). In addition to the knockdown of Smt3/SUMO, knockdown of the genes *Ubl* and *CG33223*, which encode ubiquitin-like proteins, inhibited the Dif-mediated activation of the Toll pathway (Fig. 2A), which suggests that other ubiquitin-like modifiers are involved in activating the Toll pathway.

To identify the downstream kinases of the *Drosophila* Toll pathway, we further classified the candidate protein kinases for their dependency on known signaling components (Fig. 2, B and C) and their position in the signaling hierarchy (Fig. 2D). Our analysis revealed that *Pitslre*, which encodes a *Drosophila* homolog of cyclin-dependent kinase 11b that promotes autophagic processes (*38*), was required for Toll pathway activation in all screening conditions. Furthermore, knockdown of Doa, which encodes a Cdc2-like protein kinase, also inhibited the Toll signaling pathway downstream of Pelle and Cactus. *Doa* generates at least six isoforms that localize in the cytoplasm or the nucleus, and they control broad cell processes such as germ-line development and sex determination (*39*, *40*). On the basis of the heat map view of RLA values (Fig. 2D), Pitslre and Doa appeared to be required for signaling downstream of Pelle and Cactus and upstream of Dif. These findings suggest that Pitslre and Doa are candidate downstream kinases of the Toll pathway that function between the receptor-adaptor complex and transcription factors. We also identified casein kinase Iα (CKIα) as a common factor of each screen; however, in DL1 cells, CKIα was not consistently dependent on the known signaling factors among dsRNAs with different target sequences for *CKIα*. Other kinase-encoding genes also did not satisfy the signaling hierarchy of the Toll pathway. It is possible, however, that the products of these genes specifically regulate the function of Toll, Pelle, Cactus, and Dif.

Requirement of Sherpa for host defense in adult *Drosophila*

Among these candidate genes, we focused on *sherpa/CG9153*, one of the strongest hits in the screens, as a gene encoding an uncharacterized E3 ubiquitin ligase that apparently contains a conserved E3 ligase domain. The Toll pathway is essential for the induction of genes that encode antimicrobial peptides, as well as for the survival of *Drosophila* adults upon systemic infection with Gram-positive bacteria or fungi (*41*, *42*). Consistent with the data from FlyAtlas (*43*), real-time quantitative polymerase chain reaction (qPCR) analysis indicated that *sherpa* was expressed ubiquitously, including in the fat body, the organ responsible for antimicrobial peptide production, in adult flies (fig. S2A). To analyze the role of Sherpa in host defense in adult *Drosophila*, we used a fly strain, $CG9153^{G5496}$ (referred to as $sherpa^{1}$), with a transposable P element inserted in the 5′ untranslated region (UTR) of *sherpa* (fig. S2B), which disrupts transcription of *sherpa*. The amount of *sherpa* mRNA in $sherpa^{1}$ homozygous flies was less than 20% of that in wild-type flies (fig. S2C). The $sherpa^{1}$ homozygous mutant flies were viable and fertile and had no external morphologic defects. To obtain control flies that have the same genetic background as the $sherpa^{1}$ flies, we then generated a precise excision line of *sherpa* by remobilizing the transposable P element inserted in the 5′UTR of *sherpa*. This line, referred to as $sherpa^{Rev}$, expressed a normal amount of *sherpa* mRNA (fig. S2C) and was used in addition to the Oregon R strain as a wild-type control strain in subsequent experiments. We also found that the amount of *sherpa* mRNA was constant in adult flies after systemic infection with Gram-positive bacteria (fig. S2C). Next, we examined whether $sherpa^{1}$ flies were susceptible to systemic infection. Although $sherpa^{1}$ mutant flies were resistant to saline, they rapidly succumbed to infection when challenged by some Gram-positive bacteria (Fig. 3, A to D). The $sherpa^{1}$ mutants showed no susceptibility to injection with the Gram-negative bacterium *Erwinia carotovora carotovora 15* (*Ecc15*) (Fig. 3E). The $sherpa^{Rev}$ flies showed no susceptibility to infection with Gram-positive bacteria (Fig. 3F), suggesting that increased susceptibility to Gram-positive bacteria was indeed a result of the *sherpa* mutation and not the genetic background.

We then examined whether this susceptibility to infection by Gram-positive bacteria was a result of improper Toll signaling by monitoring the expression of the antifungal peptide gene *Drs*, a target of the Toll pathway. Basal *Drs* expression in $sherpa^{1}$ mutants was not affected by saline injection (Fig. 3G) but was weakly induced by infection with the Gram-positive bacteria *S. saprophyticus* and *E. faecalis* and with the yeast *C. albicans* (Fig. 3, H to J). Lysine-type peptidoglycan, a peptidoglycan form found in most Gram-positive bacteria, potently induces Toll signaling (*44*). The $sherpa^{1}$ mutation substantially reduced the induction of *Drs* expression in flies in response to a peptidoglycan extracted from *S. aureus*, a response that was also observed in spz^{rm7} mutants (Fig. 3K). Furthermore, upon infection with *S. saprophyticus*, induction of *Drs* in flies with RNAi-mediated knockdown of Sherpa in the fat body was substantially reduced (Fig. 3L). These experiments suggested that Sherpa was required for Toll pathway activity. In contrast, the $sherpa^{1}$ mutation did not affect the expression of *Diptericin* (*Dpt*), which encodes an antibacterial peptide, upon infection with the Gram-negative bacterium *Ecc15* (Fig. 3M). The DAP-type peptidoglycan found in most Gram-negative bacteria activates the Imd pathway (*44*). The $sherpa^{1}$ mutation did not affect the induction of *Dpt* expression in response to peptidoglycan extracted from *E. coli* (Fig. 3N). Thus, our analyses of survival and antimicrobial peptide–encoding gene expression indicate a role for Sherpa in the activation of the Toll pathway by Gram-positive bacteria and fungi in *Drosophila* adults.

Epistatic analysis of Sherpa in the Toll pathway to search for the targets of Sherpa

To identify the possible targets of Sherpa, we performed an epistatic analysis of *sherpa* in Toll signaling. Overexpression of the kinase Pelle, which is downstream of dMyd88, effectively induced *Drs*-luc activity in DL1 cells (Fig. 4A). In contrast to its effects in cells in which dMyd88 was overexpressed, dsRNA-mediated knockdown of Sherpa (dsSherpa) did not suppress *Drs*-luc activity in cells in which Pelle was overexpressed (Fig. 4A and fig. S3A). Similarly, dsRNA-mediated knockdown of SUMO or of SUMO E1 and E2 enzymes did not reduce the Pelle-induced *Drs*-luc activity in DL1 cells (Fig. 4B and fig. S3B). We then tested the relationship between Sherpa and Tube, which functions upstream of Pelle and downstream of dMyd88. Pelle- or dMyd88-induced Toll pathway activation was enhanced by the combined overexpression of Tube (Fig. 4, C and D). This enhancement of *Drs*-luc activity as a result of the combined overexpression of Tube and Pelle was not reduced by knockdown of Sherpa in DL1 cells (Fig. 4C). In contrast, the enhancement of dMyd88-induced *Drs*-luc activity by Tube overexpression was reduced by knockdown of Sherpa in DL1 cells (Fig. 4D). These findings suggest that Sherpa functions upstream of Pelle and Tube and that dMyd88 could be a target of Sherpa (Fig. 4E).

Furthermore, to investigate the requirement for Sherpa and its domains in Toll signaling in DL1 cells, we made an additional dsRNA targeting the 5′ UTR region of endogenous *sherpa* mRNA and found that treatment of DL1 cells with the dsRNA also reduced dMyd88-induced *Drs*-luc activity (Fig. 4F and fig. S3C). In addition, the expression of Sherpa-FL in DL1 cells that were subjected to knockdown of Sherpa restored the normal *Drs*-luc activity that was induced by dMyd88 expression (Fig. 4F and fig. S3C). These results suggest that Sherpa was required to induce the expression of genes encoding antimicrobial peptides by the Toll pathway in cultured DL1 cells. Sherpa contains two distinct domains: the RCC repeat domain, which is a seven-bladed β propeller–like domain structurally homologous to

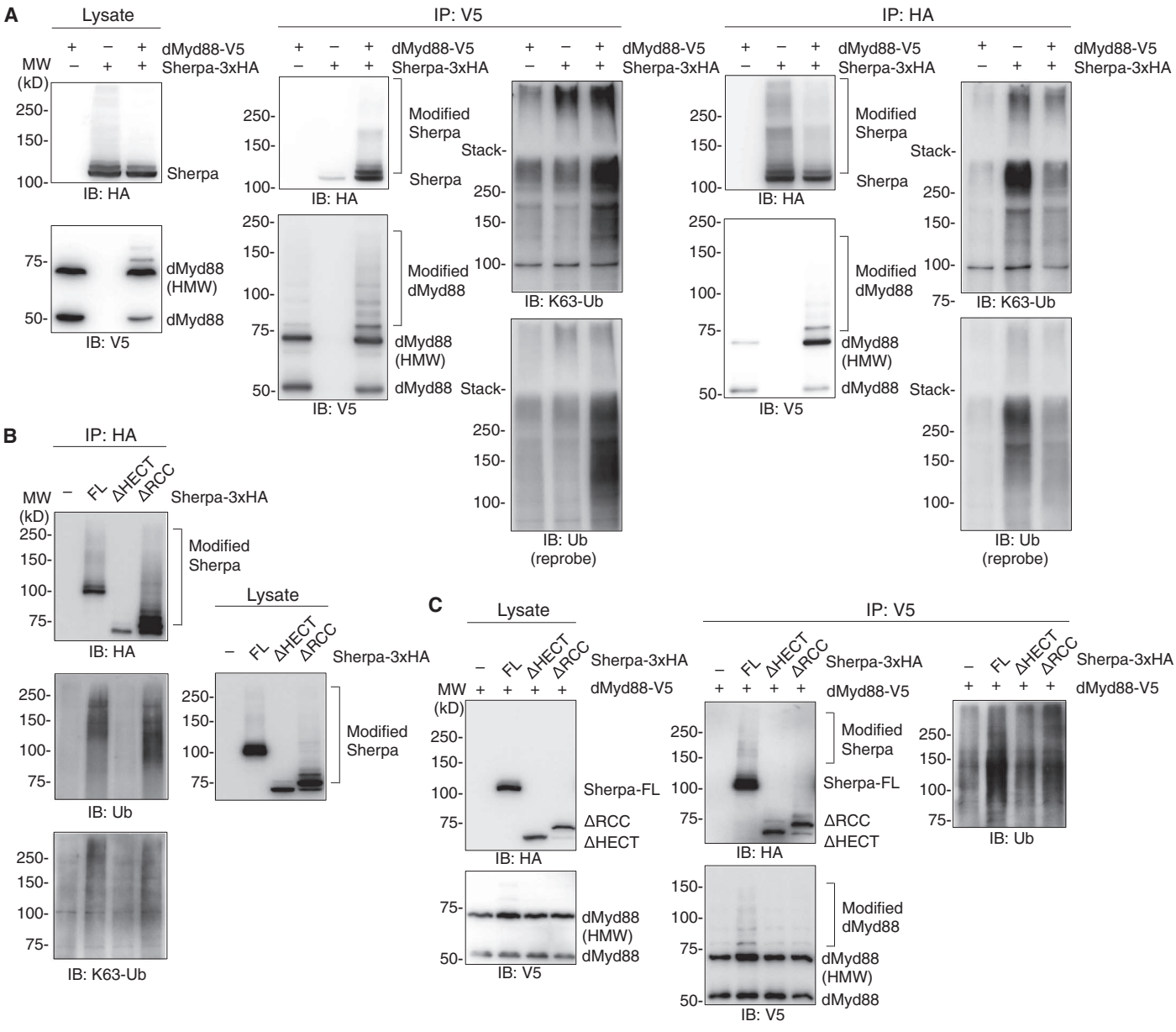

Fig. 5. Detection of physical interactions between dMyd88 and Sherpa and of posttranslational modifications, including polyubiquitylation. (**A**) DL1 cells were transfected with plasmid encoding dMyd88-V5, plasmid encoding Sherpa-3×HA, or both, and whole-cell lysates were subjected to immunoprecipitation (IP) with anti-V5 (middle) or anti-HA (right) antibodies, and both lysates and immunoprecipitated samples were subjected to Western blotting (IB) analysis with antibodies specific for the indicated proteins or tags. The polyubiquitylation of target proteins was detected with an anti-ubiquitin (Ub) antibody and a K63 linkage–specific antibody. (**B**) DL1 cells transfected with control plasmid or with expression plasmids encoding 3×HA-tagged Sherpa-FL, Sherpa-ΔHECT, or Sherpa-ΔRCC were subjected to immunoprecipitation with an anti-HA antibody, and immunoprecipitated samples and lysates were analyzed by Western blotting with antibodies against the indicated proteins. (**C**) DL1 cells transfected with control plasmid or with expression plasmid encoding dMyd88-V5 were co-transfected with expression plasmids encoding 3×HA-tagged Sherpa-FL, Sherpa-ΔHECT, or Sherpa-ΔRCC, as indicated. Cell lysates were then subjected to immunoprecipitation with an anti-V5 antibody, and immunoprecipitated samples and lysates were analyzed by Western blotting with antibodies against the indicated proteins. All Western blots are representative of at least two independent experiments. MW, molecular weight; HMW, high molecular weight.

the WD40 repeat, a domain frequently found in E3 ubiquitin ligases, and the HECT domain, which is involved in the E3 ligase activity for ubiquitylation (Fig. 4G). Rescue experiments showed that reexpression of either the RCC repeat– or the HECT domain–deficient Sherpa mutants (ΔRCC and ΔHECT, respectively) did not rescue the dMyd88-dependent induction of *Drs*-luc activity in DL1 cells in which Sherpa was knocked down (Fig. 4F),

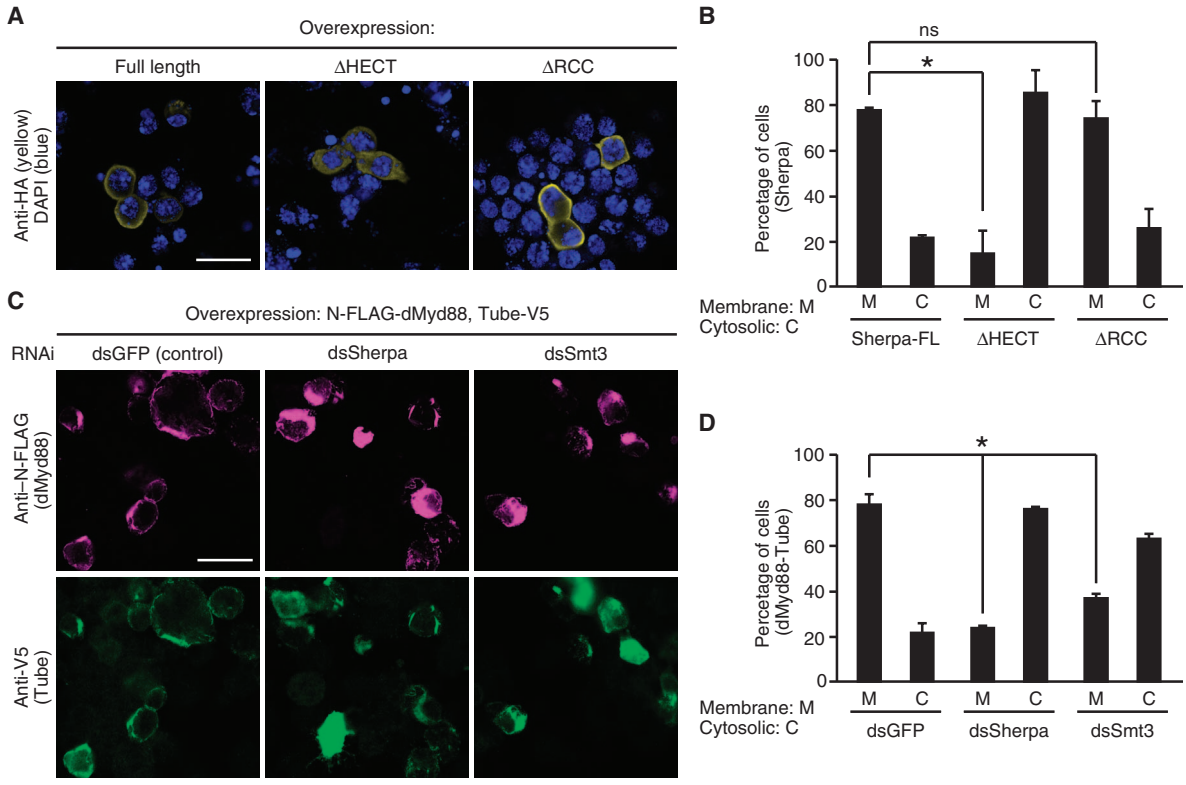

Fig. 6. Sherpa and Smt3 are required for the plasma membrane localization of the dMyd88-Tube complex in DL1 cells. (A) DL1 cells were transfected with plasmids encoding 3×HA-tagged Sherpa-FL, Sherpa-ΔHECT, or Sherpa-ΔRCC, and the subcellular localization was determined by confocal microscopy. Sherpa proteins were visualized with an anti-HA antibody. Nuclei were stained with 4′,6-diamidino-2-phenylindole (DAPI) (blue). Scale bar, 100 μm. Images are representative of three independent experiments. (B) The percentages of the cells represented in (A) that had the indicated Sherpa constructs localized to the plasma membrane as compared to the cytosol were quantified. Data are means ± SEM of three independent experiments. *$P < 0.05$ by Student's t test. (C) DL1 cells cotransfected with expression plasmids encoding FLAG-tagged dMyd88 and V5-tagged Tube proteins were also transfected with dsGFP (control), dsSherpa, or dsSmt3. The cells were then analyzed by confocal microscopy to determine the subcellular distributions of dMyd88 (red, top) and Tube (green, bottom). Scale bar, 100 μm. Images are representative of three independent experiments. (D) The percentages of the cells represented in (C) that showed plasma membrane localization of the dMyd88-Tube complex were quantified for each condition. Data are means ± SEM of three independent experiments. *$P < 0.05$ by Student's t test.

suggesting that Sherpa requires both the E3 ligase domain and the RCC domain for signaling.

Physical interactions and posttranslational modifications of dMyd88 and Sherpa

To investigate possible physical interactions between dMyd88 and Sherpa, we performed coimmunoprecipitation assays. DL1 cells were transfected with plasmids encoding C-terminal V5-tagged dMyd88 (dMyd88-V5), C-terminal 3×hemagglutinin-tagged Sherpa (Sherpa-3×HA), or both. Immunoprecipitation of dMyd88 from cell lysates followed by Western blotting analysis revealed the coimmunoprecipitation of Sherpa (Fig. 5A, middle, and fig. S4, A and B), suggesting that Sherpa physically interacts with dMyd88 in DL1 cells. A reciprocal coimmunoprecipitation assay was also indicative of a physical interaction between dMyd88 and Sherpa (Fig. 5A, right, and fig. S4, C and D).

Western blotting analysis of dMyd88 (~50 kD) in DL1 cell lysates showed double-banded signals of about 50 and 70 kD in size, and in lysates of cells coexpressing Sherpa, the dMyd88-specific bands shifted to 70 kD as well as higher molecular mass forms greater than 70 kD (Fig. 5A, left). Immunoprecipitated dMyd88 from cells coexpressing Sherpa showed multiple bands corresponding to modified proteins ranging from 75 to >150 kD in size (Fig. 5A, middle, and fig. S4, E to G). Sherpa also showed evidence of multiple posttranslational modifications, which broadly ranged from 100 kD to the maximum molecular mass (Fig. 5A). These results implied that Sherpa mediated and promoted multiple posttranslational modifications of dMyd88 and of Sherpa itself. Western blotting analysis showed increasing polyubiquitination signals, including K63-linked polyubiquitin chains, in lysates from cells overexpressing Sherpa (Fig. 5A and fig. S4, H and I), which suggests that Sherpa generates polyubiquitin chains on Sherpa and dMyd88.

We then investigated the requirement of the domains of Sherpa for polyubiquitination in experiments with the domain deletion mutants of Sherpa. Immunoprecipitation and Western blotting analysis of Sherpa constructs from transfected DL1 cells showed that Sherpa-FL and Sherpa-ΔRCC, but not Sherpa-ΔHECT, showed polyubiquitylation signals, including K63-linked polyubiquitin chains (Fig. 5B), suggesting that the HECT domain has E3 ubiquitin ligase activity and is required for the autoubiquitylation of Sherpa. Furthermore, a coimmunoprecipitation experiment with cells coexpressing dMyd88 with domain deletion mutants of Sherpa showed that Sherpa-ΔHECT and Sherpa-ΔRCC both failed to induce modifications of

dMyd88 (Fig. 5C), consistent with the results of the rescue experiments in DL1 cells (Fig. 4F). These findings suggest that Sherpa functions as an E3 ubiquitin ligase for dMyd88 and that it contributes to Toll pathway signaling, which is dependent not only on its HECT domain but also on its RCC repeat region. Additionally, we investigated the involvement of Smt3/SUMO in the modifications of dMyd88 and Tube. First, we found that polyubiquitylation of Tube, including by K63-linked ubiquitin chains, was induced in cells coexpressing dMyd88 (fig. S5A). We then found that the amount of K63-ubiquitylated proteins in the immunoprecipitated dMyd88-Tube complex was further increased by the overexpression of Smt3-GG, an activated mutant of Smt3 (fig. S5, A and B). Consistent with the results of the epistatic analysis (fig. 4B), these findings also suggest that SUMO enhances Toll pathway signaling by dMyd88.

Regulation of the plasma membrane localization of the dMyd88-Tube complex by Sherpa and SUMO

We next analyzed the subcellular localization of Sherpa in DL1 cells. Confocal microscopic imaging of Sherpa-FL in DL1 cells and quantitative analysis showed that Sherpa mainly localized near the inner surface of the plasma membrane (Fig. 6, A and B), suggesting that Sherpa functions near the plasma membrane where dMyd88 associates and functions. To identify the domain of Sherpa required for its membrane localization, we analyzed the subcellular localization of domain deletion mutants of Sherpa. Immunostaining experiments indicated that Sherpa-ΔHECT failed to associate with the plasma membrane but was dispersed in the cytosol (Fig. 6, A and B). In contrast, deletion of the RCC repeat region from Sherpa did not affect its membrane localization (Fig. 6, A and B). These findings suggested that Sherpa localizes to the plasma membrane through its HECT domain, which is also required for the autoubiquitylation of Sherpa and its modifications of dMyd88.

On the basis of these results, we assessed the requirement for Sherpa in the membrane localization of dMyd88 and Tube. Immunostaining and quantitative analysis (Fig. 6, C and D) showed that dMyd88 and Tube colocalized at the plasma membrane in control knockdown DL1 cells but failed to localize at the plasma membrane in DL1 cells in which Sherpa was knocked down; instead, they formed aggregates in the cytosol. These results suggest that Sherpa mediates the proper membrane localization of the dMyd88-Tube complex that is essential for Toll pathway signaling. Moreover, Smt3 knockdown DL1 cells also showed improper membrane localization of the dMyd88-Tube complex, similarly to that found in Sherpa knockdown DL1 cells (Fig. 6, C and D).These findings suggest that both Sherpa and Smt3 are required for plasma membrane localization of the dMyd88-Tube complex and that they contribute to appropriate complex formation and signaling.

Involvement of the protein kinases Pitslre and Doa in Toll pathway activation

In addition to ubiquitin and SUMO-related factors, we tested whether the protein kinases Pitslre and Doa regulated the Toll signaling pathway in adult flies. We measured the expression of *Drosomycin* mRNA in the RNAi-induced knockdown flies after bacterial infection. Fat body–directed knockdown of the Cdc2-related protein kinase Pitslre (fig. S6A) attenuated *Drosomycin* expression after infection with the Gram-positive bacterium *S. saprophyticus* (fig. S6B). Knockdown of Pitslre, however, also reduced the expression of *Diptericin*, which encodes an antimicrobial peptide and is strictly regulated by the Imd pathway, after infection by the Gram-negative bacterium *Ecc15* (fig. S6C). Thus, we speculate that Pitslre regulates common signaling processes, such as the regulation of nuclear components or the proper development and maintenance of innate immune cells and organs. Additionally, we confirmed the involvement of the Cdc2-like protein kinase Doa in the Toll signaling pathway in DL1 cells. Knockdown of Doa by dsRNA (fig. S6D), which targeted a sequence common to all Doa isoforms, critically inhibited activation of the Toll pathway in cells overexpressing either dMyd88 or Pelle (fig. S6, E and F). Because the gene encoding Doa generates multiple isoforms that have distinct functions (*39*, *40*), the specific isoform of Doa that is required for Toll pathway signaling must be determined in future studies.

DISCUSSION

Although the Toll pathway is the main signaling pathway responsible for the innate immune response in *Drosophila*, the mechanisms of Toll intracellular signaling are not as well elucidated as those of the mammalian TLR pathway. Intriguingly, several components of the mammalian TLR pathway, for example, TAK1 and IKK, function in the *Drosophila* Imd pathway but have no function in the Toll pathway, suggesting that previously uncharacterized molecules are involved in intracellular Toll signaling.

To begin this study, we first successfully identified DL1 cells as an optimal cell line in which conventional Toll signaling is entirely preserved. DL1 cells also had excellent transfection efficiency, making them quite suitable for large-scale screening that required multiple transfection components such as expression vectors and reporter genes. Here, we performed ex vivo, genome-wide RNAi screening with DL1 cells to identify the signaling molecules of the Toll pathway, and we demonstrated that SUMO and the E3 ubiquitin ligase Sherpa were required for intracellular Toll pathway signaling ex vivo and in vivo. This finding was supported by four lines of evidence: (i) the expression of *Drosomycin* induced by dMyd88 overexpression was abolished by the knockdown of *sherpa*; (ii) this effect of *sherpa* knockdown in DL1 cells was rescued by the expression of Sherpa-FL but not of a mutant Sherpa deficient in the E3 ligase domain; (iii) the loss-of-function *sherpa* mutant failed to activate the Toll pathway in response to either Gram-positive bacteria or yeast; and (iv) in vivo RNAi silencing of *sherpa* in the fat body also compromised the activation of the Toll pathway. In addition, epistatic analyses in DL1 cells suggested that Sherpa functions in parallel with dMyd88.

Protein modification by SUMO is emerging as an important post-translational modification for regulating signal transduction (*45*, *46*). The *Drosophila* genome encodes only one SUMO polypeptide, in contrast to the four known SUMO isoforms in vertebrates. Similar to the process of ubiquitylation, SUMO is covalently attached to the ε-amino group of certain lysine residues in substrate proteins. SUMOylation normally involves a conserved cascade consisting of the heterodimeric E1-activating enzyme complex Aos1-Uba2 in *Drosophila* (SAE1-SAE2 in mammals), the E2-conjugating enzyme Ubc9, and an E3 ligase. Our RNAi screening data suggested the involvement of all these E1 and E2 enzymes in activating the Toll pathway (Fig. 2A).

In TLR signaling and TNF-α signaling in mammals, the E3 ubiquitin ligases of the TRAF and cIAP families are involved in complex formation and the ubiquitylation of their upstream adaptor kinase proteins, such as IRAKs and RIPKs. Autoubiquitylation of these E3 ligases is also critical for their own activation and for the recruitment of downstream components, such as the E3 ubiquitin ligase complex LUBAC and the IKK complex. In Imd signaling, Diap2, the *Drosophila* ortholog of cIAP, mediates the ubiquitylation of Imd, an adaptor protein homologous to the RIPKs, which induces downstream signaling events. Our immunoprecipitation assay indicated that Sherpa physically interacted with the adaptor protein dMyd88 and that it induced multiple posttranslational modifications of dMyd88, including ubiquitylation through its HECT domain. Furthermore, Sherpa also induced its own K63-linked polyubiquitylation through the HECT domain. Immunocytochemical analysis indicated that Sherpa was localized at the plasma membrane through the HECT domain, and both Sherpa and SUMO were

critically required for the plasma membrane localization of the dMyd88-Tube complex in DL1 cells, which is required for proper signaling complex formation near the plasma membrane and Toll. Thus, our analysis suggests that Sherpa is a previously uncharacterized signaling component in the Toll pathway that controls the subcellular localization of the dMyd88-Tube complex through posttranslational modifications and that it is required for host defense in the adult *Drosophila*. It remains elusive, however, how and why ubiquitylation or SUMOylation were required for the subcellular localization of the dMyd88-Tube complex. The detailed relationship between the modification and subcellular localization of this adaptor complex should be determined in future studies by identifying the modification sites of dMyd88 and Tube. It is possible that the K63-linked polyubiquitylation chains on Sherpa are also required for recruitment of uncharacterized downstream components into the signaling complex that consists of dMyd88 and Tube.

Additionally, we also confirmed the involvement of protein kinase genes *Pitslre* and *Doa* in Toll pathway activation. *Pitslre* was required for Toll pathway activation in *Drosophila* adults after infection by Gram-positive bacteria. *Doa* was essential to Toll pathway signaling downstream of dMyd88 and Pelle in DL1 cells. These results suggest that *Pitslre* and *Doa* facilitate downstream signaling in the Toll pathway and phosphorylate the IκB protein Cactus and NF-κB protein Dif.

Together, the results of our comparative genome-wide screening and in vivo studies provide information regarding the molecular mechanisms involved in intracellular Toll signaling. These findings will help to elucidate the molecular basis of the intracellular Toll pathway.

MATERIALS AND METHODS

Cell culture

DL1 cells were obtained from the DRSC (Harvard Medical School) and maintained at 25°C in Schneider's *Drosophila* medium (Invitrogen) containing 10% (v/v) heat-inactivated fetal bovine serum and 1× antibiotic-antimycotic (Life Technologies).

Vector construction

The complementary DNA (cDNA) fragments encoding full-length *Drosophila* MyD88 (dMyd88), Tube, Pelle, and Dif were amplified with KOD -Plus- version 2 DNA polymerase (Toyobo) and subcloned into a pMT-V5His expression vector (Invitrogen) at the Kpn I and Xho I sites. The Torso-Tube construct was generated as previously described, with modifications (*47*, *48*). The cDNA fragments encoding Torso (nucleotides 1 to 1358) with a Kpn I site at the 5′ end and a BstE II site at the 3′ end, and full-length Tube with the BstE II site at the 5′ end and the Xho I site at the 3′ end were fused and subcloned into the pMT-V5His vector. For Sherpa/CG9153 constructs, cDNA fragments for the full-length protein (Met^{1} to Val^{1058}) and the ΔRCC [Met (start codon)–Asp^{380} to Val^{1058}] and ΔHECT (Met^{1} to Phe^{700}) mutants were amplified together with the C-terminal 3×HA tag sequence by PCR and subcloned into the pUAST vector at the Xho I/Sal I and Kpn I sites. The cDNA fragments of dMyd88 and Pelle with the Xho I site at the 5′ end and the Kpn I site at the 3′ end were also subcloned into the pUAST vector together with the N-terminal FLAG tag sequence [Met (start codon)–Asp–Tyr–Lys–Asp–Asp–Asp–Asp–Lys]. The cDNA fragment encoding dMyd88-V5His in the pMT-V5His vector was also subcloned into the pUAST vector at the Xho I/Sal I and Kpn I sites. The cDNA fragment encoding Smt3-GG was amplified by PCR together with the N-terminal HA tag sequence and a stop codon after Gly^{88} and was subcloned into the pMT-V5His at the Kpn I and Xho I sites. The pMT-GAL4 vector was provided by the Drosophila Genomics Resource Center (stock no. 1042). To generate the pGL3–*Drosomycin*–firefly luciferase reporter vector, the promoter region of *Drosomycin* (NCBI Reference Sequence: NT_037436.4; 3367189–3369621) was subcloned into the pGL3 vector (Promega). To generate the pAc5.1–*Renilla* luciferase transfection control vector, the DNA fragment of *hRluc* and the SV40 polyadenylation signal sequence on pGL4.70 was cleaved at the Xho I site at the 5′ end and the Bam HI site at the 3′ end, and then directly cloned into the pAc5.1 vector using the same restriction enzyme sites.

Genome-wide RNAi screening and analysis

We used the DRSC Genome-Wide RNAi Library (DRSC 2.0), 66 × 384-well microplates with dsRNAs covering ~13,900 genes, for the genome-wide RNAi screening. *Drosophila* DL1 cells were transfected with vectors and dsRNA with Effectene Transfection reagent (Qiagen) as follows. Each well of each 384-well plate contained 10 ng of pGL3–*Drosomycin*–firefly luciferase reporter vector, 10 ng of pAc5.1–*Renilla* luciferase transfection control vector, 0.4 μl of Enhancer, and 0.5 μl of Effectene diluted in 9.3 μl of buffer EC. In addition, 10 ng of pMT-dMyd88, 0.4 ng of pMT-Pelle, and 1.0 ng of pMT-Dif or 10 ng of dsRNA specific for Cactus were supplied for each screen. The solution (~10 μl) was immediately mixed with 80 ng of dsRNA in each well of the screening plate. After a 10-min incubation, 35 μl of DL1 cells (1.0×10^{6} cells/ml) was transfected with the lipid-nucleotide complex in the well and cultured at 28°C for 24 hours. Overexpression was induced by adding $CuSO_4$ at a final concentration of 0.5 mM for 48 hours. Firefly luciferase activity (*Drosomycin* promoter activity) and *Renilla* luciferase activity (cell viability and transfection efficiency) were measured with a SpectraMax L-TYA luminometer (Molecular Devices) with the Dual-Glo Luciferase Assay System (Promega). The data analysis was performed according to the median + *k* median absolute deviation method, as described previously (*49*). RLAs (firefly/*Renilla*) were calculated and transformed to a percentage of the median RLA in each plate.

dsRNA synthesis

DNA fragments of the target genes were amplified by PCR to contain a T7-RNA polymerase promoter at the 5′ and 3′ ends. Sequences of the PCR primers are shown in table S1. Single-stranded RNAs were synthesized with T7 RNA polymerase (Roche), and annealed dsRNAs were purified and precipitated in ethanol (*6*). Each dsRNA was dissolved in ribonuclease-free water and stored at −30°C.

RNAi and luciferase reporter assay

DL1 cells (1.0×10^{5} in 100 μl) were plated in 96-well plates and transfected with 100 ng of dsRNA, 100 ng of pGL3–*Drosomycin*–firefly luciferase reporter vector, and 20 ng of pAc5.1–*Renilla* luciferase transfection control vector, together with the expression vectors indicated in the figure legends, using the Effectene transfection reagent (2.0 μl of Enhancer and 2.5 μl of Effectene diluted in 20.5 μl of buffer EC; Qiagen).Twenty-four hours after transfection, expression was induced by adding $CuSO_4$ to a final concentration of ~1.0 mM, and the cells were incubated at 28°C for a further 24 hours. Luciferase activity was measured with the Dual-Glo Luciferase Assay System (Promega) with a SpectraMax L-TYA luminometer (Molecular Devices), as described earlier.

Immunoprecipitation and Western blotting

A 6-ml scale-up culture of DL1 cells expressing either the C-terminal dMyd88-V5 (encoded by pUAST-dMyd88-V5His), the C-terminal Sherpa-3×HA (encoded by pUAST-Sherpa-3×HA), or both was lysed in 500 μl of lysis buffer [50 mM tris-HCl (pH 7.5), 150 mM NaCl, 1 mM EDTA, 5% glycerol, 1% NP-40] supplemented with Complete protease inhibitor cocktail (EDTA-free; Roche) and incubated at 4°C for 1 hour to solubilize

the proteins. The insoluble proteins were removed by centrifugation at 14,000*g* for 5 min at 4°C. The dMyd88-V5 proteins were immunoprecipitated from the cell lysate with 1.0 μg of anti-V5 mouse monoclonal antibody (Invitrogen) and 35 μl of a slurry of Dynabeads Sheep Anti-Mouse Immunoglobulin G (IgG; Invitrogen) overnight at 4°C. The N-terminal FLAG–tagged dMyd88 (N-FLAG-dMyd88) proteins were also immunoprecipitated from the cell lysate with 1.0 μg of anti-DYKDDDDK (2H8) mouse monoclonal antibody (Transgenic) and 35 μl of a slurry of Dynabeads Sheep Anti-Mouse IgG (Invitrogen) overnight at 4°C. In the reciprocal immunoprecipitation assay, the Sherpa-3×HA proteins were immunoprecipitated from the cell lysate with 0.2 μg of rat monoclonal anti-HA antibody (3F10; Roche) and 40 μl of a slurry of Dynabeads Protein G (Invitrogen) overnight at 4°C. The beads were washed three times in 500 μl of lysis buffer. Precipitated proteins on the beads were eluted in 30 μl of 1× Laemmli sample buffer and were denatured and reduced by boiling at 95°C for 5 min. Proteins were resolved by SDS–polyacrylamide gel electrophoresis with an 8% resolving gel and a 5% stacking gel using the Mini-Protean Tetra Cell system (Bio-Rad) and then were transferred to a polyvinylidene difluoride membrane (GE Healthcare Life Sciences) with the Mini Trans-Blot system (Bio-Rad). Membranes were incubated in blocking buffer [50 mM tris-HCl (pH 7.5), 150 mM NaCl, 0.1% Tween 20, 5% skim milk] at room temperature for 2 to 3 hours and then were incubated with primary antibodies in blocking buffer. The dMyd88-V5 proteins in cell lysates and those immunoprecipitated from cell lysates were detected with an anti-V5 mouse monoclonal antibody (Invitrogen) and an anti-V5 rabbit polyclonal antibody (MBL), respectively. The Sherpa-3×HA proteins in cell lysates and those coimmunoprecipitated from cell lysates were detected with an anti-HA (3F10) rat monoclonal antibody (Roche). The N-FLAG-dMyd88 proteins were detected with an anti-DYKDDDDK (2H8) mouse monoclonal antibody (Transgenic). Ubiquitylated proteins were detected with a horseradish peroxidase (HRP)–conjugated anti-ubiquitin mouse monoclonal antibody (P4D1; Cell Signaling). K63-linked ubiquitin chains were detected with a K63 linkage–specific anti-polyubiquitin (D7A11) rabbit monoclonal antibody (Cell Signaling) using Can Get Signal Immunoreaction Enhancer Solution (Toyobo). Subsequently, membranes were treated with peroxidase-linked secondary antibodies (GE Healthcare Life Science) at room temperature for 2 hours, and the signals were detected by Luminata Forte Western HRP substrate (Merck Millipore) with the ImageQuant LAS 400 mini system (GE Healthcare Life Science). Western blotting data were analyzed by densitometry with ImageQuant TL software (GE Healthcare Life Science).

Immunocytochemistry

Cells (2.0×10^5 in 200 μl) were transfected with plasmids: 150 ng of pMT-GAL4, 75 ng of pUAST-FLAG-dMyd88, 75 ng of pMT-Tube-V5His, and 250 ng of dsRNA, or 150 ng of pMT-GAL4 and 150 ng of pUAST-Sherpa-FL or domain-deficient mutant–3×HA with the Effectene transfection reagent (5.0 μl of Enhancer and 7.5 μl of Effectene diluted in 75 μl of buffer EC; Qiagen) in a four-well chamber slide (BD Falcon), and protein production was induced by 1 mM $CuSO_4$. The cells were rinsed in saline (Otsuka) and fixed in 4% paraformaldehyde in phosphate-buffered saline (PBS) for 30 min. The fixative was removed by washing three times with PBS, and the cells were permeabilized in PBS-T [0.3% (v/v) Triton X-100] for 30 min, followed by blocking in 5% (w/v) bovine serum albumin (BSA) in PBS-T for 30 min. Cells were incubated with primary antibodies in 5% (w/v) BSA–PBS-T overnight at 4°C. The cells were then washed three times in PBS-T and incubated with secondary antibodies (Jackson ImmunoResearch) for 3 hours and then with DAPI for 20 min at room temperature, which was followed by mounting with Vectashield (Vector Laboratories). Image sampling was performed with a confocal microscopy system (Leica). For quantitative analysis, about 100 cells were counted for each sample, and the percentage of the cells that had membrane-bound signal was determined.

Fly stocks used in this study

Drosophila stocks were maintained in standard cornmeal-yeast-agar medium vials at 25°C. Oregon R and *yw* flies were used as wild-type controls. As a positive control for the Toll susceptible lines, spz^{rm7} flies (*50*) were used, and for Imd susceptibility, $Relish^{E20}$ flies (*51*) were used as a positive control. *yw;P{EP}CG9153*^{G5486}, P element inserted flies designated *CG9153/sherpa*^{1} were provided by the Bloomington Drosophila Stock Center (stock no. 27181). The revertant line *CG9153/sherpa*^{Rev} was generated by excision of the P element with flies from *yw;P{EP}CG9153*^{G5486}. Pitslre-RNAi transgenic flies were provided by the Vienna Drosophila Resource Center (stock no. 107303). *lacZ*-expressing flies, Toll-RNAi, Sherpa-RNAi, and Pitslre-RNAi using *UAS-Dcr2;c564-GAL4* flies were crossed at 18°C and moved to 28°C after eclosion.

Pathogens, peptidoglycans, microbial infection, and survival experiments

The following pathogens were used for infection: *C. albicans* (NBRC1385), *Ecc15* (IFO3830), *E. faecalis* (IFO12964), and *S. saprophyticus* (GTC0205). The following peptidoglycans were used: PGN-SA (peptidoglycan from *S. aureus*, InvivoGen catalog no. tlrl-pgnsa) and PGN-EK (peptidoglycan from *E. coli K12*-TLR2 ligand, InvivoGen catalog no. tlrl-pgnek). Flies (3 to 7 days after eclosion) were infected by being injected with a suspension of each pathogen strain (70 nl per fly). The optical density at 600 nm for each suspension was 1.0 for *Ecc15* and 0.1 for *S. saprophyticus*. For survival experiments, we used ~30 flies of each genotype at 28°C. Surviving flies were counted daily while being transferred to fresh vials.

Total RNA isolation and qPCR analysis

Flies were infected as described earlier or were injected with peptidoglycans (10 μg/ml, 70 nl per fly) and were collected at 24 hours (*S. saprophyticus*) or 6 hours (*Ecc15*). Total RNAs were isolated from 10 flies of each genotype with TRIzol reagent (Ambion). Total RNA (1 mg) was used for cDNA synthesis with ReverTra Ace reverse transcriptase (Toyobo) and oligo$(dT)_{15}$ primer (Promega). With first-strand cDNA (0.5 μl), qPCR was performed with a LightCycler (Roche Diagnostics). *rpL32* was used as the internal control. The following primers were used for qPCR: *rpL32*, AGATCGTGAAGAAGCGCACCAAG (forward) and CACCAGGAACTTCTTGAATCCGG (reverse); *Drs*, TTGTTCGCCCTCTTCGCTGTCCT (forward) and GCATCCTTCGCACCAGCACTTCA (reverse); *Dpt*, GTTCACCATTGCCGTCGCCTTAC (forward) and CCAAGTGCTGTCCATATCCTCC (reverse); *Herc*, CGTCGAGCTGCACTACAATGC (forward) and GTATCATCGACCGAAGTGTAGC (reverse); *Smt3*, AAGCAAAAGGAAGCCGCTTG (forward) and TGTTGAAGCTGCTAAGTGGTC (reverse); *Pitslre*, TCGCCGAATTCTTGCAGATG (forward) and GCGACAACATGTTCTTCACG (reverse); and *Doa*, ATGGAGGTGCTGGCTTCTTC (forward) and TAAACGCGTGCACTTGGAAG (reverse).

Statistical analysis

Statistical analysis was performed with the Student's *t* test or the log-rank test, as appropriate. A P value of <0.05 was considered to be statistically significant.

SUPPLEMENTARY MATERIALS

www.sciencesignaling.org/cgi/content/full/8/400/ra107/DC1

Fig. S1. Numbers of candidate genes for each screening sorted by functional annotations.

Fig. S2. Expression profiles of *sherpa* and the *sherpa*^{1} loss-of-function mutant.

Fig. S3. Knockdown efficiency of *sherpa* and *smt3* in DL1 cells.
Fig. S4. Quantification of coimmunoprecipitated proteins and posttranslational modifications, including polyubiquitylation.
Fig. S5. Western blotting analysis of Tube coexpressed with dMyd88 and Smt3.
Fig. S6. Expression of *Drosomycin* and *Diptericin* mRNAs in PitsIre-RNAi flies and analysis of *Drosomycin* promoter activity in Doa-RNAi cells.
Table S1. Sequences of DNA primers used for dsRNA synthesis.
Data file S1. List of candidate genes for each screening sorted by functional annotation.

REFERENCES AND NOTES

1. A. Goto, K. Matsushita, V. Gesellchen, L. El Chamy, D. Kuttenkeuler, O. Takeuchi, J. A. Hoffmann, S. Akira, M. Boutros, J.-M. Reichhart, Akirins are highly conserved nuclear proteins required for NF-κB-dependent gene expression in drosophila and mice. *Nat. Immunol.* **9**, 97–104 (2008).
2. S. E. Mohr, J. A. Smith, C. E. Shamu, R. A. Neumüller, N. Perrimon, RNAi screening comes of age: Improved techniques and complementary approaches. *Nat. Rev. Mol. Cell Biol.* **15**, 591–600 (2014).
3. S. Cherry, Genomic RNAi screening in *Drosophila* S2 cells: What have we learned about host–pathogen interactions? *Curr. Opin. Microbiol.* **11**, 262–270 (2008).
4. D. Ferrandon, J. L. Imler, C. Hetru, J. A. Hoffmann, The *Drosophila* systemic immune response: Sensing and signalling during bacterial and fungal infections. *Nat. Rev. Immunol.* **7**, 862–874 (2007).
5. B. Lemaitre, J. Hoffmann, The host defense of *Drosophila melanogaster*. *Annu. Rev. Immunol.* **25**, 697–743 (2007).
6. A. Goto, T. Yano, J. Terashima, S. Iwashita, Y. Oshima, S. Kurata, Cooperative regulation of the induction of the novel antibacterial Listericin by peptidoglycan recognition protein LE and the JAK-STAT pathway. *J. Biol. Chem.* **285**, 15731–15738 (2010).
7. A. Kleino, N. Silverman, The *Drosophila* IMD pathway in the activation of the humoral immune response. *Dev. Comp. Immunol.* **42**, 25–35 (2014).
8. H. Myllymäki, S. Valanne, M. Rämet, The *Drosophila* Imd signaling pathway. *J. Immunol.* **192**, 3455–3462 (2014).
9. P. Georgel, S. Naitza, C. Kappler, D. Ferrandon, D. Zachary, C. Swimmer, C. Kopczynski, G. Duyk, J.-M. Reichhart, J. A. Hoffmann, *Drosophila* immune deficiency (IMD) is a death domain protein that activates antibacterial defense and can promote apoptosis. *Dev. Cell* **1**, 503–514 (2001).
10. N. Paquette, M. Broemer, K. Aggarwal, L. Chen, M. Husson, D. Erturk-Hasdemir, J. M. Reichhart, P. Meier, N. Silverman, Caspase-mediated cleavage, IAP binding, and ubiquitination: Linking three mechanisms crucial for *Drosophila* NF-κB signaling. *Mol. Cell* **37**, 172–182 (2010).
11. N. Silverman, R. Zhou, S. Stöven, N. Pandey, D. Hultmark, T. Maniatis, A *Drosophila* IκB kinase complex required for Relish cleavage and antibacterial immunity. *Genes Dev.* **14**, 2461–2471 (2000).
12. S. Stöven, N. Silverman, A. Junell, M. Hedengren-Olcott, D. Erturk, Y. Engström, T. Maniatis, D. Hultmark, Caspase-mediated processing of the *Drosophila* NF-κB factor Relish. *Proc. Natl. Acad. Sci. U.S.A.* 100, 5991–5996 (2003).
13. I.-H. Jang, N. Chosa, S.-H. Kim, H.-J. Nam, B. Lemaitre, M. Ochiai, Z. Kambris, S. Brun, C. Hashimoto, M. Ashida, P. T. Brey, W.-J. Lee, A Spätzle-processing enzyme required for Toll signaling activation in *Drosophila* innate immunity. *Dev. Cell* **10**, 45–55 (2006).
14. L. El Chamy, V. Leclerc, I. Caldelari, J.-M. Reichhart, Sensing of 'danger signals' and pathogen-associated molecular patterns defines binary signaling pathways 'upstream' of Toll. *Nat. Immunol.* **9**, 1165–1170 (2008).
15. N. Buchon, M. Poidevin, H.-M. Kwon, A. Guillou, V. Sottas, B.-L. Lee, B. Lemaitre, A single modular serine protease integrates signals from pattern-recognition receptors upstream of the *Drosophila* Toll pathway. *Proc. Natl. Acad. Sci. U.S.A.* **106**, 12442–12447 (2009).
16. A. N. R. Weber, S. Tauszig-Delamasure, J. A. Hoffmann, E. Lelièvre, H. Gascan, K. P. Ray, M. A. Morse, J.-L. Imler, N. J. Gay, Binding of the *Drosophila* cytokine Spätzle to Toll is direct and establishes signaling. *Nat. Immunol.* **4**, 794–800 (2003).
17. S. Tauszig-Delamasure, H. Bilak, M. Capovilla, J. A. Hoffmann, J.-L. Imler, *Drosophila* MyD88 is required for the response to fungal and Gram-positive bacterial infections. *Nat. Immunol.* **3**, 91–97 (2002).
18. P. Towb, R. L. Galindo, S. A. Wasserman, Recruitment of Tube and Pelle to signaling sites at the surface of the Drosophila embryo. *Development* **125**, 2443–2450 (1998).
19. H. Sun, P. Towb, D. N. Chiem, B. A. Foster, S. A. Wasserman, Regulated assembly of the Toll signaling complex drives *Drosophila* dorsoventral patterning. *EMBO J.* **23**, 100–110 (2004).
20. J. Daigneault, L. Klemetsaune, S. A. Wasserman, The IRAK homolog Pelle is the functional counterpart of IκB kinase in the *Drosophila* Toll pathway. *PLOS One* **8**, e75150 (2013).
21. M. P. Belvin, Y. Jin, K. V. Anderson, Cactus protein degradation mediates *Drosophila* dorsal-ventral signaling. *Genes Dev.* **9**, 783–793 (1995).
22. M. Reach, R. L. Galindo, P. Towb, J. L. Allen, M. Karin, S. A. Wasserman, A gradient of cactus protein degradation establishes dorsoventral polarity in the *Drosophila* embryo. *Dev. Biol.* **180**, 353–364 (1996).
23. Y. T. Ip, M. Reach, Y. Engstrom, L. Kadalayil, H. Cai, S. González-Crespo, K. Tatei, M. Levine, *Dif*, a *dorsal*-related gene that mediates an immune response in Drosophila. *Cell* **75**, 753–763 (1993).
24. P. Manfruelli, J.-M. Reichhart, R. Steward, J. A. Hoffmann, B. Lemaitre, A mosaic analysis in *Drosophila* fat body cells of the control of antimicrobial peptide genes by the Rel proteins Dorsal and DIF. *EMBO J.* **18**, 3380–3391 (1999).
25. O. Takeuchi, S. Akira, Pattern recognition receptors and inflammation. *Cell* **140**, 805–820 (2010).
26. T. Kawagoe, S. Sato, K. Matsushita, H. Kato, K. Matsui, Y. Kumagai, T. Saitoh, T. Kawai, O. Takeuchi, S. Akira, Sequential control of Toll-like receptor–dependent responses by IRAK1 and IRAK2. *Nat. Immunol.* **9**, 684–691 (2008).
27. R. G. Baker, M. S. Hayden, S. Ghosh, NF-κB, inflammation, and metabolic disease. *Cell Metab.* **13**, 11–22 (2011).
28. S. Roth, Y. Hiromi, D. Godt, C. Nusslein-Volhard, *cactus*, a maternal gene required for proper formation of the dorsoventral morphogen gradient in *Drosophila* embryos. *Development* **112**, 371–388 (1991).
29. S. Valanne, H. Myllymäki, J. Kallio, M. R. Schmid, A. Kleino, A. Murumägi, L. Airaksinen, T. Kotipelto, M. Kaustio, J. Ulvila, S. S. Esfahani, Y. Engström, O. Silvennoinen, D. Hultmark, M. Parikka, M. Rämet, Genome-wide RNA interference in *Drosophila* cells identifies G protein-coupled receptor kinase 2 as a conserved regulator of NF-κB signaling. *J. Immunol.* **184**, 6188–6198 (2010).
30. R. Steward, Dorsal, an embryonic polarity gene in Drosophila, is homologous to the vertebrate proto-oncogene, c-rel. *Science* **238**, 692–694 (1987).
31. D. E. Reed, X. M. Huang, J. A. Wohlschlegel, M. S. Levine, K. Senger, DEAF-1 regulates immunity gene expression in *Drosophila*. *Proc. Natl. Acad. Sci. U.S.A.* **105**, 8351–8356 (2008).
32. D. Kuttenkeuler,N. Pelte, A. Ragab, V. Gesellchen, L. Schneider, C. Blass, E. Axelsson, W. Huber, M. Boutros, A large-scale RNAi screen identifies *Deaf1* as a regulator of innate immune responses in *Drosophila*. *J. Innate Immun.* **2**, 181–194 (2010).
33. L. Mandal, U. Banerjee, V. Hartenstein, Evidence for a fruit fly hemangioblast and similarities between lymph-gland hematopoiesis in fruit fly and mammal aorta-gonadal-mesonephros mesoderm. *Nat. Genet.* **36**, 1019–1023 (2004).
34. A. Kleino, S. Valanne, J. Ulvila, J. Kallio, H. Myllymäki, H. Enwald, S. Stöven, M. Poidevin, R. Ueda, D. Hultmark, B. Lemaitre, M. Rämet, Inhibitor of apoptosis 2 and TAK1-binding protein are components of the *Drosophila* Imd pathway. *EMBO J.* **24**, 3423–3434 (2005).
35. W. Huang da, B. T. Sherman, R. A. Lempicki, Systematic and integrative analysis of large gene lists using DAVID bioinformatics resources. *Nat. Protoc.* **4**, 44–57 (2008).
36. W. Huang da, B. T. Sherman, R. A. Lempicki, Bioinformatics enrichment tools: Paths toward the comprehensive functional analysis of large gene lists. *Nucleic Acids Res.* **37**, 1–13 (2009).
37. Q. Huang, X. Tang, G. Wang, Y. Fan, L. Ray, A. Bergmann, T. Y. Belenkaya, X. Ling, D. Yan, Y. Lin, X. Ye, W. Shi, X. Zhou, F. Lu, J. Qu, X. Lin, Ubr3 E3 ligase regulates apoptosis by controlling the activity of DIAP1 in Drosophila. *Cell Death Differ.* **21**, 1961–1970 (2014)
38. S. Wilkinson, D. R. Croft, J. O'Prey, A. Meedendorp, M. O'Prey, C. Dufès, K. M. Ryan, The cyclin-dependent kinase PITSLRE/CDK11 is required for successful autophagy. *Autophagy* **7**, 1295–1301 (2011).
39. B. Yun, K. Lee, R. Farkas, C. Hitte, L. Rabinow, The LAMMER protein kinase encoded by the *Doa* locus of Drosophila is required in both somatic and germline cells and is expressed as both nuclear and cytoplasmic isoforms throughout development. *Genetics* **156**, 749–761 (2000).
40. A. Kpebe, L. Rabinow, Dissection of darkener of apricot kinase isoform functions in Drosophila. *Genetics* **179**, 1973–1987 (2008).
41. T. Michel, J.-M. Reichhart, J. A. Hoffmann, J. Royet, *Drosophila* Toll is activated by Gram-positive bacteria through a circulating peptidoglycan recognition protein. *Nature* **414**, 756–759 (2001).
42. M. Gottar, V. Gobert, A. A. Matskevich, J.-M. Reichhart, C. Wang, T. M. Butt, M. Belvin, J. A. Hoffmann, D. Ferrandon, Dual detection of fungal infections in *Drosophila* via recognition of glucans and sensing of virulence factors. *Cell* **127**, 1425–1437 (2006).
43. V. R. Chintapalli, J. Wang, J. A. T. Dow, Using FlyAtlas to identify better *Drosophila melanogaster* models of human disease.*Nat. Genet.* **39**, 715–720 (2007).
44. F. Leulier, C. Parquet, S. Pili-Floury, J.-H. Ryu, M. Caroff, W.-J. Lee, D. Mengin-Lecreulx, B. Lemaitre, The *Drosophila* immune system detects bacteria through specific peptidoglycan recognition. *Nat. Immunol.* **4**, 478–484 (2003).
45. X.-J. Yang, C.-M. Chiang, Sumoylation in gene regulation, human disease, and therapeutic action. *F1000Prime Rep.* **5**, 45 (2013).
46. A. Flotho, F. Melchior, Sumoylation: A regulatory protein modification in health and disease. *Annu. Rev. Biochem.***82**, 357–385 (2013).
47. R. L. Galindo, D. N. Edwards, S. K. Gillespie, S. A. Wasserman, Interaction of the pelle kinase with the membrane-associated protein tube is required for transduction of the dorsoventral signal in *Drosophila* embryos. *Development* **121**, 2209–2218 (1995).
48. H. Sun, B. N. Bristow, G. Qu, S. A. Wasserman, A heterotrimeric death domain complex in Toll signaling. *Proc. Natl. Acad. Sci. U.S.A.* **99**, 12871–12876 (2002).

49. A. Birmingham, L. M. Selfors, T. Forster, D. Wrobel, C. J. Kennedy, E. Shanks, J. Santoyo-Lopez, D. J. Dunican, A. Long, D. Kelleher, Q. Smith, R. L. Beijersbergen, P. Ghazal, C. E. Shamu, Statistical methods for analysis of high-throughput RNA interference screens. *Nat. Methods* **6**, 569–575 (2009).
50. D. Morisato, K. V. Anderson, The *spätzle* gene encodes a component of the extracellular signaling pathway establishing the dorsal-ventral pattern of the Drosophila embryo. *Cell* **76**, 677–688 (1994).
51. M. Hedengren, B. Åsling, M. S. Dushay, I. Ando, S. Ekengren, M. Wihlborg, D. Hultmark, *Relish*, a central factor in the control of humoral but not cellular immunity in *Drosophila*. *Mol. Cell* **4**, 827–837 (1999).

Acknowledgments: We are grateful to the Bloomington Drosophila Stock Center, the Drosophila Genomics Resource Center at Indiana University, the Drosophila Genetic Resource Center at the Kyoto Institute of Technology, the DRSC, the Genetic Strain Research Center of National Institute of Genetics, and the Vienna Drosophila RNAi Center for fly stocks. **Funding:** This work was supported by grants from the Japan Science and Technology Agency; the Ministry of Education, Culture, Sports, Science, and Technology of Japan; the Program for the Promotion of Basic Research Activities for Innovative Biosciences; a Global COE Research Grant (Tohoku University Ecosystem Adaptability); the Takeda Science Foundation; the Kao Foundation for Arts and Sciences; the Uehara Memorial Foundation; and the Futaba Electronics Memorial Foundation. **Author contributions:** H.K. and T.K. conceived this study; H.K., T.K., and L.-L.T. designed the experiments; H.K. and L.-L.T. performed many of the experiments with input from T.K. and H.K.; H.K. performed genome-wide ex vivo RNAi screenings and bioinformatics analysis; L.-L.T. and F.S. performed genetic crosses and fly studies; H.K. and L.-L.T. performed the reporter assays in cultured *Drosophila* cells; H.K. and Y.S. performed immunoprecipitations, Western blotting, and immunocytochemical analysis; L.-L.T. and Y.M. performed qPCR analysis; H.K., L.-L.T., and Y.M. performed subcloning, dsRNA synthesis, cell culture, and transfections; T.K., H.K., L.-L.T., Y.S., and Y.M. analyzed the data; H.K., L.-L.T., and T.K. wrote the Introduction, Results, figure legends, and Discussion and compiled the references; H.K. and L.-L.T. wrote the Materials and Methods and Supplementary Materials and prepared the figures; H.K., L.-L.T., T.K., and S.K. completed the manuscript; T.K. managed and controlled this project with help from H.K.; and S.K. oversaw the study. **Competing interests:** The authors declare that they have no competing interests. **Data and materials availability:** Data from the *Drosophila* RNAi screens have been deposited in the DRSC (http://www.flyrnai.org/).

Submitted 29 September 2014
Accepted 9 October 2015
Final Publication 27 October 2015
10.1126/scisignal.2005971
Citation: H. Kanoh, L.-L. Tong, T. Kuraishi, Y. Suda, Y. Momiuchi, F. Shishido, S. Kurata, Genome-wide RNAi screening implicates the E3 ubiquitin ligase Sherpa in mediating innate immune signaling by Toll in *Drosophila* adults. *Sci. Signal.* **8**, ra107 (2015).

Genome-wide RNAi screening implicates the E3 ubiquitin ligase Sherpa in mediating innate immune signaling by Toll in *Drosophila* adults

Hirotaka Kanoh, Li-Li Tong, Takayuki Kuraishi, Yamato Suda, Yoshiki Momiuchi, Fumi Shishido and Shoichiro Kurata

Sci. Signal. **8** (400), ra107.
DOI: 10.1126/scisignal.2005971

Sherpa guides Toll signaling

Mammalian Toll-like receptors (TLRs) recognize pathogen-derived molecular patterns and stimulate the innate immune response. These proteins are named for their counterparts in the fruit fly *Drosophila* in which the first of these, Toll, was identified. Kanoh *et al*. showed that the fly Toll innate immune signaling pathway required an E3 ubiquitin ligase called Sherpa. Flies expressing a ligase-defective mutant Sherpa had compromised immune responses to bacterial infection. The adaptor protein dMyd88, which interacts with Toll, relied on both Sherpa and the *Drosophila* SUMO homolog for proper subcellular localization. Thus, this study reveals additional similarities between the fly and mammalian innate immune systems.